nature chemistry

ARTICLES

PUBLISHED ONLINE: 15 JANUARY 2018 | DOI: 10.1038/NCHEM.2917

Engineered modular biomaterial logic gates for environmentally triggered therapeutic delivery

Barry A. Badeau[1], Michael P. Comerford[1], Christopher K. Arakawa[2], Jared A. Shadish[1] and Cole A. DeForest[1,2,3,4]*

The successful transport of drug- and cell-based therapeutics to diseased sites represents a major barrier in the development of clinical therapies. Targeted delivery can be mediated through degradable biomaterial vehicles that utilize disease biomarkers to trigger payload release. Here, we report a modular chemical framework for imparting hydrogels with precise degradative responsiveness by using multiple environmental cues to trigger reactions that operate user-programmable Boolean logic. By specifying the molecular architecture and connectivity of orthogonal stimuli-labile moieties within material cross-linkers, we show selective control over gel dissolution and therapeutic delivery. To illustrate the versatility of this methodology, we synthesized 17 distinct stimuli-responsive materials that collectively yielded all possible YES/OR/AND logic outputs from input combinations involving enzyme, reductant and light. Using these hydrogels we demonstrate the first sequential and environmentally stimulated release of multiple cell lines in well-defined combinations from a material. We expect these platforms will find utility in several diverse fields including drug delivery, diagnostics and regenerative medicine.

Recent innovations in therapeutic development and cell engineering have yielded powerful tools to combat an increasing number of debilitating and life-threatening diseases. Despite these advances, several barriers to clinical translation remain, including the significant challenge of limiting therapeutic deployment to sites of disease that can be widespread and unknown[1–4]. Targeted delivery strategies that exploit disease-related biomarkers improve treatment efficiency and efficacy by reducing dosage requirements and adverse off-target effects[4–8]. Most typically, these methods employ polymer-based vehicles to facilitate delivery and protect therapeutic cargo from immune recognition, clearance and non-specific cellular uptake. Cell-based therapies further necessitate that these vehicles recapitulate critical aspects of native tissue to ensure sustained cell viability and function. Hydrogels offer promise in each of these regards, as they are robust material platforms whose biochemical and biophysical properties can be tuned to preserve and promote specific cell fates, are readily formulated into a variety of shapes and stiffnesses to control transport to and within tissues, and can be engineered to degrade in response to locally presented cues to facilitate therapeutic release[9,10].

Smart materials have been engineered to leverage pathophysiology for targeted delivery by integrating functional groups that cleave or change conformation in response to an external stimulus (for example, enzyme, pH, temperature, redox conditions and small molecules), allowing them to sense and respond to disease-associated biochemical hallmarks[3,4,7]. Although materials sensitive to single factors can enrich therapeutic delivery to sites of disease, individual biomarkers are rarely unique to these locations, leading to suboptimal selectivity. For example, cancer microenvironments have been targeted through their extensive matrix metalloproteinase (MMP) activity, reducing conditions and subphysiological pH. However, these characteristics are shared, respectively, by healthy joints[11], the intracellular milieu[4] and the stomach. To improve the site specificity of payload release, materials that degrade only when presented with multiple cues have been developed[3,12–19]. While previous approaches have enabled therapeutic delivery in response to two environmental factors, they lack a generalizable framework to exploit additional input stimuli to further refine release specificity. Moreover, the uniqueness of each previously reported responsive platform necessitates a complete material redesign—one that is generally not synthetically tractable due to inherent constraints on material composition and vehicle geometry—in order to alter the response profiles or utilize different biochemical triggers. Furthermore, the subset of degradable materials demonstrated for live cell release has been limited to single biological inputs[20–23], confining next-generation cellular therapeutics to simple delivery platforms.

To address these technological limitations and enable unprecedented specificity over controlled therapeutic release, we sought to develop a versatile chemistry-based approach to create multi-stimuli-responsive hydrogel platforms that are (1) able to perform biocomputation, (2) modular in design and (3) fully cytocompatible. Biocomputation represents the ability to simultaneously sense multiple biologically presented inputs and follow a user-programmed Boolean logic-based algorithm to provide a functional output[7], demonstrated here in the form of material degradation and therapeutic delivery. System modularity allows both the inputs and logic functions to be changed and combined to generate a theoretically limitless number of novel materials, each with unique and user-specified release characteristics. Furthermore, exploitation of cytocompatible bioorthogonal chemistries permits responsive material platforms to be formed and degraded on demand in the presence of live cells, representing a major improvement over existing cell delivery strategies.

In our rational design-based approach, stimuli-sensitive components are incorporated into discrete, monodisperse, synthetic

[1]Department of Chemical Engineering, University of Washington, Seattle, WA 98195, USA. [2]Department of Bioengineering, University of Washington, Seattle, WA 98105, USA. [3]Institute of Stem Cell & Regenerative Medicine, University of Washington, Seattle, WA 98109, USA. [4]Molecular Engineering & Sciences Institute, University of Washington, Seattle, WA 98195, USA. *e-mail: profcole@uw.edu

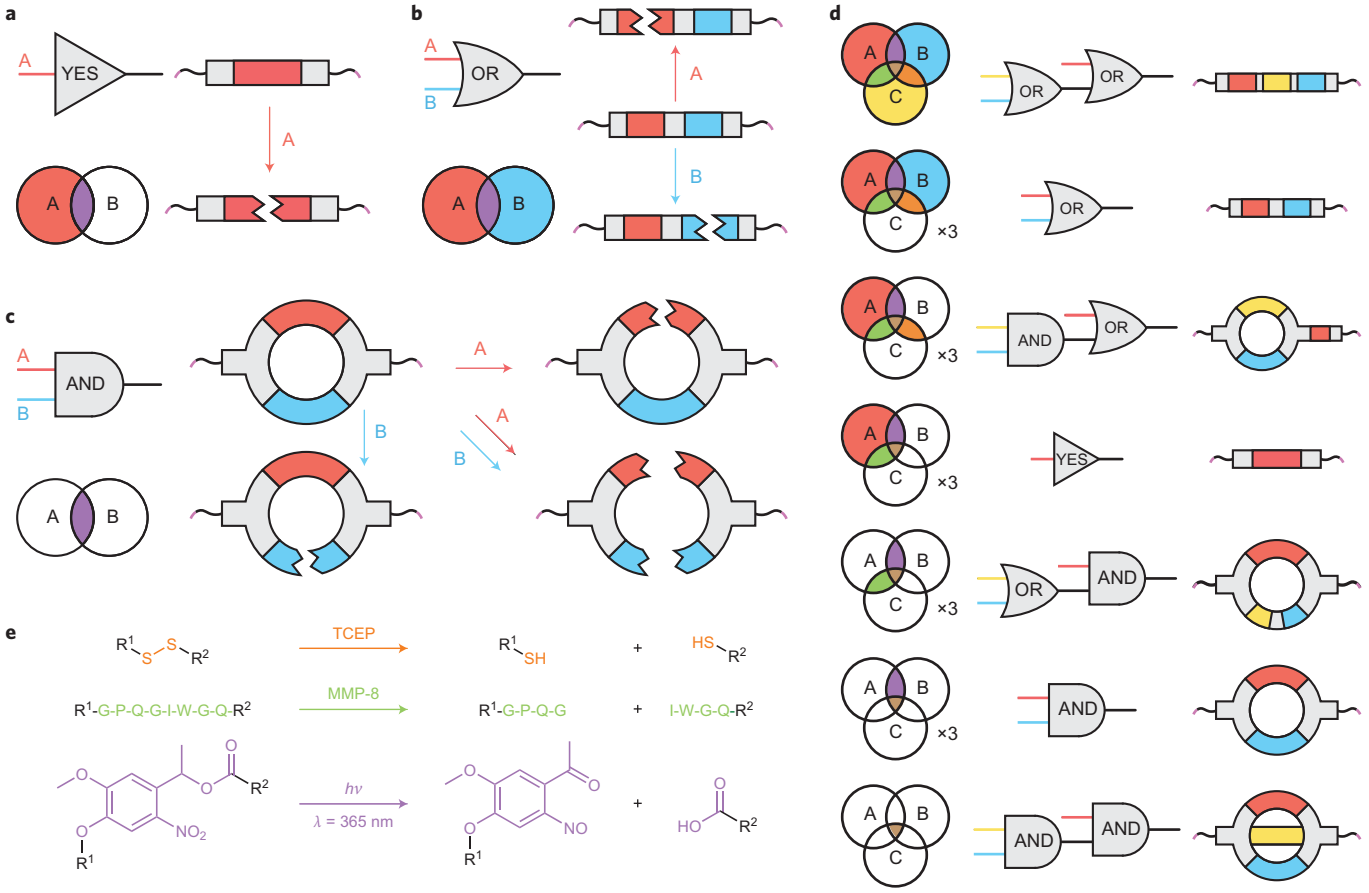

Figure 1 | Rationally designed cross-linker architecture enables logic-based material degradation. a, The YES-gate material cross-linker contains a single stimuli-labile moiety (red). Presence of the corresponding chemical input cleaves this moiety, breaking the covalent linkage between molecular endpoints (pink) to yield material degradation. Each region of the Venn diagram corresponds to a unique combination of inputs and indicates whether the material is expected to degrade (coloured) or remain intact (light grey). **b**, The OR-gate cross-linker contains two different stimuli-labile moieties (red and blue) connected in series. The presence of either relevant input cleaves the cross-linker, resulting in material degradation. **c**, The AND-gate cross-linker contains two different stimuli-labile moieties (red and blue) connected in parallel. The presence of a single programmed input cleaves one linker arm but does not fully sever the crosslink, leaving material crosslinking density and mechanical properties unchanged. **d**, Logic gates can be hierarchically combined to generate higher-order logic responses. Seventeen unique materials can be generated by combining three logic gates (YES, OR, AND) with three distinct inputs. **e**, Reactions depicting cleavage of the stimuli-labile groups: disulfide bonds (orange) are reduced into free thiols, the proteolytically sensitive peptide sequence GPQG↓IWGQ (green) is enzymatically cleaved by MMP, and the *o*NB moiety (purple) undergoes photoscission in the presence of near-UV light (λ = 365 nm).

cross-linkers that, upon reaction with polymer macromers, form hydrogels of well-defined molecular architecture. Information governing the environmental responsiveness of the resulting material is embedded within the cross-linker domain; when the linker is covalently cleaved, the material degrades and simultaneously releases any encapsulated or tethered payload. The simplest Boolean logic function, the YES gate, is implemented when a single stimuli-labile moiety is included in the linker. We hypothesized that more advanced logic operations could be built through the controlled connectivity of additional cleavable groups within a cross-linker. When two degradable units are connected in series, the cleavage of either moiety causes material dissolution, forming an OR gate (denoted with logic symbol $\vee$). When two degradable units are connected in parallel, the cleavage of both moieties is required for material dissolution, forming an AND gate (denoted by logic symbol $\wedge$). These concepts can be expanded hierarchically, combining multiple gates into a logic circuit to engineer complex responses to additional dynamic stimuli (Fig. 1). Formalizing the relationship between cross-linker architecture and hydrogel degradability provides a template for creating materials that are structurally simple yet functionally complex.

Results

Synthesis of logic-based responsive cross-linkers. Implementation of the outlined biocomputational strategy requires precise control over cross-linker functionality and architecture. We used peptide-based cross-linkers due to the efficiency of solid-phase peptide synthesis in generating monodisperse macromolecules that contain a range of functional groups with sequence-defined order and connectivity. Peptides, which possess intrinsic biocompatibility, can be chemically modified to introduce non-canonical functionality, connectivity (for example, branching, cyclization and intramolecular stapling) and degradability. As a demonstration of this logic-based approach, three chemically orthogonal stimuli-labile moieties from different reaction classes were employed: (1) the enzymatically degradable oligopeptide sequence, GPQG↓IWGQ, which cleaves in the presence of MMPs and allows for a cell- and disease-triggered response[24]; (2) disulfide bonds, which degrade under reducing conditions present both intracellularly and in disease states; and (3) an *ortho*-nitrobenzyl ester (*o*NB), which undergoes photoscission upon cytocompatible near-ultraviolet (near-UV) light exposure (λ = 365 nm), thereby facilitating user-defined spatiotemporal

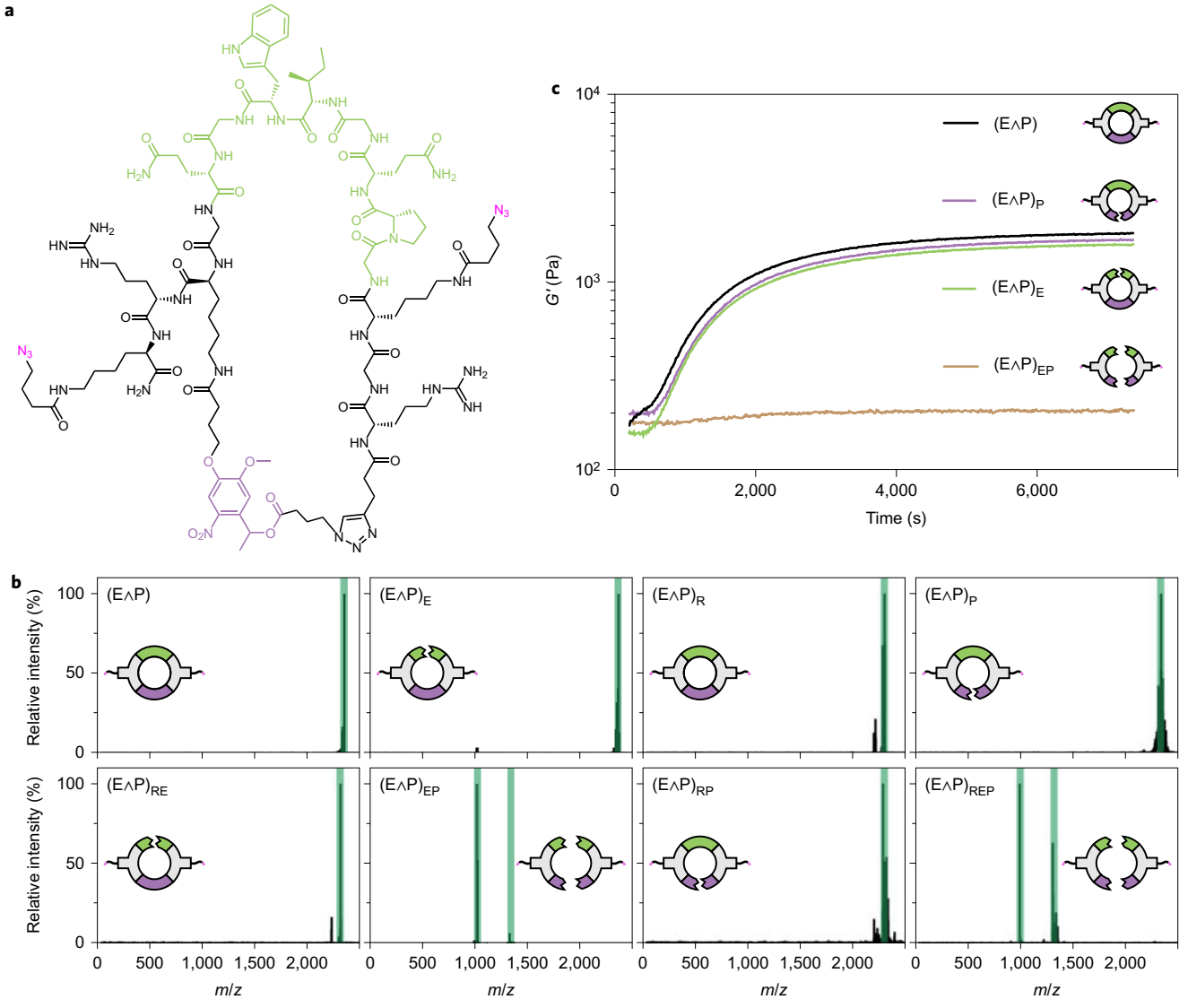

Figure 2 | Engineered cross-linkers respond to environmental input combinations on the molecular level. a, The chemical structure of the E∧P cross-linker includes an MMP-degradable peptide sequence (green), a photolabile oNB moiety (purple), and two flanking azides (pink) for SPAAC-based hydrogel crosslinking. **b**, MALDI-TOF spectra of the E∧P cross-linker after treatment with all unique combinations of enzyme ($_E$), reductive species ($_R$) and light ($_P$) demonstrate correct molecular responses following each input combination. Expected product masses are highlighted in green. **c**, *In situ* oscillatory rheological analysis of hydrogels crosslinked using treated E∧P demonstrates that AND-gated materials require treatment by both relevant inputs to yield changes in bulk material properties.

control over material properties[25] (Fig. 1e). Exhaustively spanning all hierarchical YES/OR/AND combinations of these three stimuli-labile moieties, we synthesized 17 distinct cross-linkers that each exhibit a unique logic output (Supplementary Methods 1–21). Each cross-linker was flanked with two reactive azide moieties to enable the formation of nearly ideal step-growth hydrogel networks by means of a strain-promoted, azide–alkyne cycloaddition (SPAAC) reaction[26] with four-arm poly(ethylene glycol) tetrabicyclononyne (PEG-tetraBCN; Supplementary Methods 22). SPAAC click chemistry rapidly produces homogeneous hydrogels in a bioorthogonal fashion, thereby permitting encapsulation of bioactive therapeutics and living cells[27–29]. Moreover, an extensive toolbox of SPAAC-compatible modifications allows for uniform network functionalization with moieties ranging from small molecules to full-length proteins[29–32]. Such tunability further enables the design of complex delivery vehicles, for example, through the inclusion of targeting moieties, instructive cues to guide encapsulated cell fate and function, or tethered therapeutics to be released upon material dissolution.

Assessing solution-based cross-linker degradation in response to environmental stimuli. To demonstrate that cross-linkers degrade as engineered in response to environmental cues and that stimuli-responsive reactions are chemically orthogonal, we treated each of the one- and two-input linkers with every possible combination of MMP enzyme ($_E$), reducing conditions ($_R$) and light ($_P$) (Supplementary Methods 23 and 24). Reaction products were characterized using matrix-assisted laser desorption/ionization time-of-flight mass spectrometry (MALDI–TOF). Detected masses were in excellent agreement with those of the expected reaction products (Fig. 2 and Supplementary Figs 1–9), indicating that the linkers respond as designed on a molecular level. To further investigate, the enzyme AND photolinker (E∧P) was pretreated with different combinations of enzyme and light, added to a stoichiometrically defined amount of PEG-tetraBCN, and

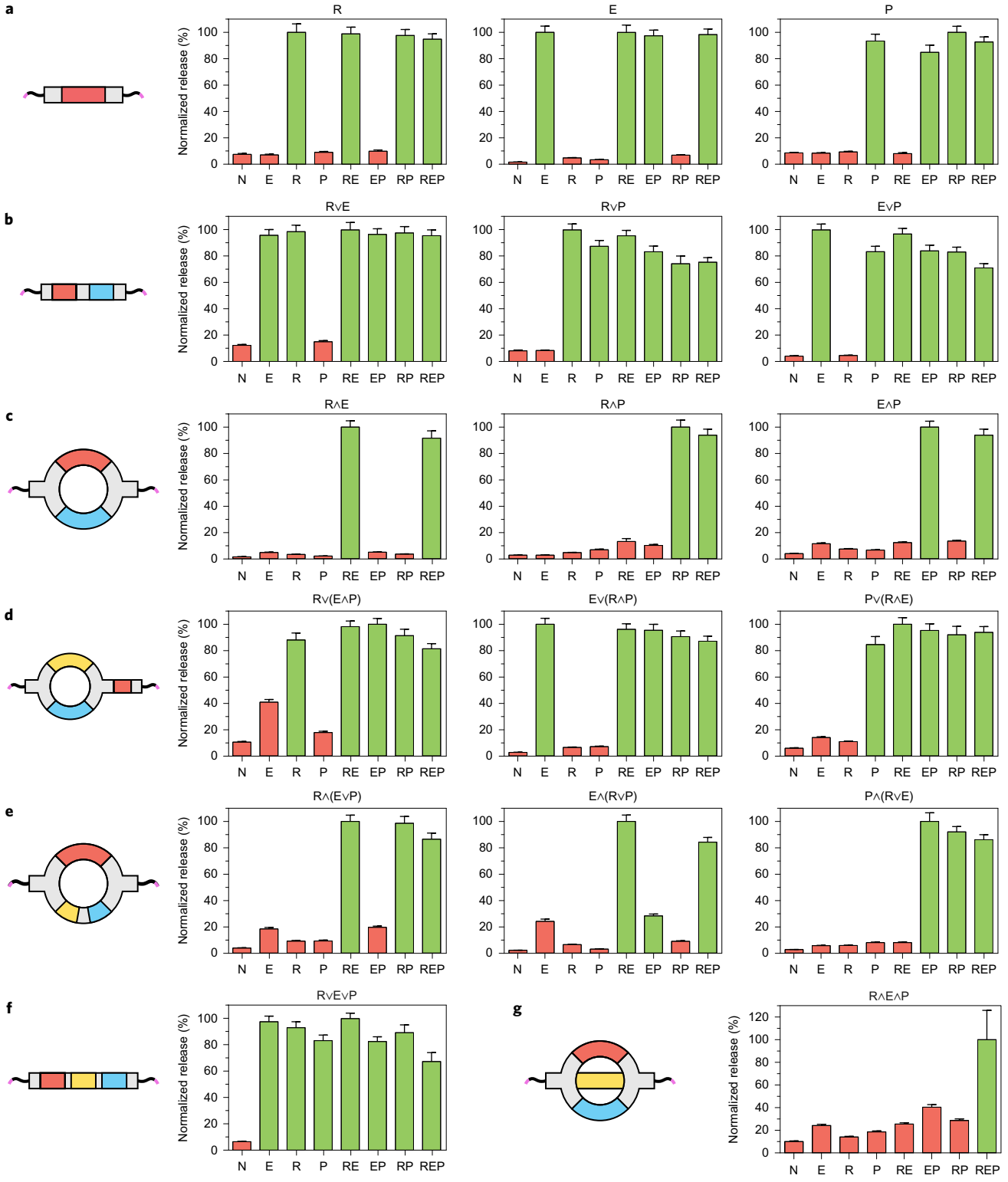

Figure 3 | Logic-gated biomaterials exhibit programmable degradation in response to environmentally presented input combinations. a, The response profiles of the single-input YES-gated materials. **b**,**c**, Response profiles of the two-input OR-gated (**b**) and AND-gated (**c**) materials. **d**–**g**, Response profiles of the higher-order, three-input OR/(AND)- (**d**), AND/(OR)- (**e**), OR/OR- (**f**) and AND/AND- (**g**) gated materials. Plot titles correspond to cross-linker identity, with *x*-axis labels indicating material treatment conditions ($_N$ indicates no treatment, $_E$ is MMP enzyme, $_R$ is a chemical reductant, $_P$ is UV light). Green bars signify conditions expected to result in material degradation; red bars indicate conditions expected not to yield material degradation. Error bars correspond to ±1 standard deviation about the mean with propagated uncertainties for $n = 3$ experimental replicates.

characterized by *in situ* oscillatory rheology to monitor evolution of material properties (Supplementary Methods 22 and 25). Untreated EʌP yielded robust gels, demonstrating the first successful use of a cyclic or stapled peptide for material crosslinking. The final storage moduli of samples containing the untreated linker ($G' = 1{,}660 \pm 170$ Pa) were similar to those of the linkers subjected

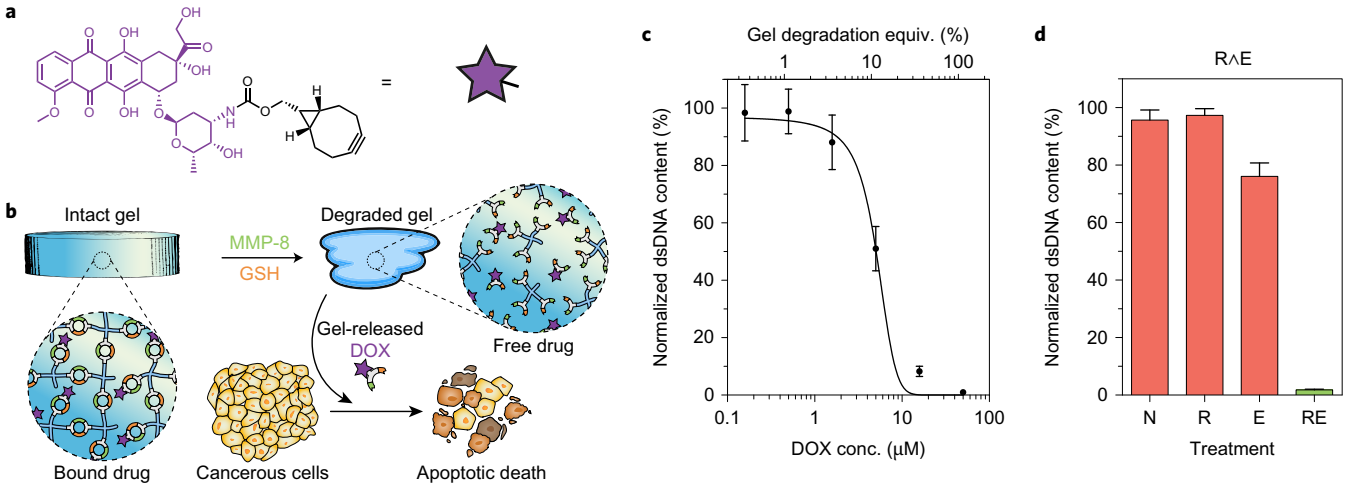

Figure 4 | Logic-based doxorubicin delivery enhances specificity of HeLa cell death in the presence of multiple disease-state hallmarks. a, Chemical structure of doxorubicin functionalized at the amino group with BCN. **b**, RΛE hydrogel degradation is triggered in the presence of pathophysiological cues associated with tumour microenvironments: reducing conditions and MMPs. Liberated DOX induces apoptosis in cervical cancer-derived HeLa cells. **c**, Dose–response curve of HeLa cells following treatment with RΛE–DOX conjugate. **d**, Normalized dsDNA content after culturing HeLa with released hydrogel components following varying treatments. *x*-axis label indicates material treatment conditions: $_N$ is no treatment, $_R$ is a chemical reductant, $_E$ is MMP enzyme. The green bar signifies conditions expected to result in DOX release though material degradation. Red bars indicate conditions expected not to yield material degradation. Error bars correspond to ±1 standard deviation about the mean for $n = 3$ experimental replicates.

to either enzyme or light ($G' = 1{,}580 \pm 130$ Pa and $1{,}540 \pm 110$ Pa, respectively), while the linker treated with both enzyme and light did not form a gel ($G' = 200 \pm 30$). All samples had a final loss modulus (G'') of ~50 Pa. Consistent with rubber elasticity theory where the shear modulus scales with crosslinking density[33] and calculations showing that distances between network branch points increase ≤3% upon cleavage of a single arm of AND-gated linkers (Supplementary Methods 26), these data suggest that the mechanical properties of these materials depend only on the final logic state of the Boolean linker.

Logic-based hydrogel degradation in response to environmental stimuli. After validating linker behaviour on the molecular level, we sought to characterize the logic-based stimuli-responsiveness of bulk materials. Each cross-linker was reacted independently with Alexa568-labelled PEG-tetraBCN to form 17 different types of fluorescent hydrogel. For each type, responsiveness to all eight input combinations involving reducing agents, light and enzyme was evaluated. Hydrogel degradation was quantified by measuring supernatant fluorescence at non-kinetically limited endpoints following treatment (Fig. 3, Supplementary Methods 27 and 28 and Supplementary Figs 10 and 11). Each of the YES-gated materials (E, R and P) behaved as expected, degrading only when the programmed cue was present. The high selectivity (more than tenfold over non-specific release) again demonstrates the orthogonality of the employed stimuli-labile chemistries. The OR-gated materials (RvE, EvP, RvP) also responded as expected, degrading fully when either of the relevant cues was present. The AND-gated materials (RΛE, EΛP, RΛP) also functioned properly, fully degrading only when both programmed cues were present. The observed release selectivity (more than sevenfold) is as or more specific than the most successful dual-input degradable materials previously reported[12,14–16]. Of the three-input materials containing two logic gates, six of eight (that is, Ev(RΛP), Pv(RΛE), RΛ(EvP), PΛ(RvE), RvEvP, Rv(EΛP)) behaved fully as designed, degrading with high selectivity only when the respective cues were present. The conditions $(E\Lambda(R\vee P))_{EP}$ and $(R\Lambda E\Lambda P)_{REP}$ did not fully degrade, which we attribute to the known decreased proteolytic cleavage kinetics for strained MMP-degradable substrates[34], in this case due to internal ring strain. These higher-order, three-input cross-linkers are the most complex logic operators ever used to control material degradation. This generalizable approach proves robust, as 132 of the 136 treatment conditions yielded engineered degradation (defined as either complete degradation or <30% nonspecific release). The exhaustive synthesis and testing of each possible material demonstrates that complex biomaterial computation can be achieved with high fidelity through the hierarchical combination of simple YES/OR/AND logic gates. Given the initial success of this modular framework, we expect to be able to substitute the chosen stimuli-labile groups with any number of other chemically orthogonal moieties sensitive to pH, additional proteases, visible light, temperature or ultrasound.

Disease-associated delivery of doxorubicin to an *in vitro* cancer model. To demonstrate the ability to deliver functional therapeutics in response to precise combinations of pathophysiological stimuli, we tethered a BCN-tagged doxorubicin (DOX) chemotherapeutic into RΛE gels that degrade with high specificity to cancer microenvironmental cues (Fig. 4a,b and Supplementary Methods 29). The extent of hydrogel functionalization was chosen such that the solution DOX concentration following full material degradation (44 μM) would yield population-wide apoptotic death of plated cervical cancer-derived HeLa cells (Fig. 4c). Following treatment by each relevant input combination (that is, $_N$, $_E$, $_R$, $_{RE}$), cells were incubated in hydrogel supernatants for 48 h before quantitative analysis of double-stranded DNA (dsDNA) content, indicative of the total number of viable cells. In the absence of treatment, or that with just reductant or MMP, normal proliferation was observed (95 ± 3%, 97 ± 2% and 76 ± 5%, respectively, relative to non-treated controls lacking gels). The slight decrease in total dsDNA content following enzymatic treatment is attributed to secondary effects of the MMP treatment, rather than to non-specific DOX release (Supplementary Methods 29). In stark contrast to treatments with a single input, treatment with both inputs resulted in complete cell eradication (1.8 ± 0.2% dsDNA content relative to controls), as designed. These results highlight the unique capacity of this approach to control the release of functional small-molecule therapeutics through

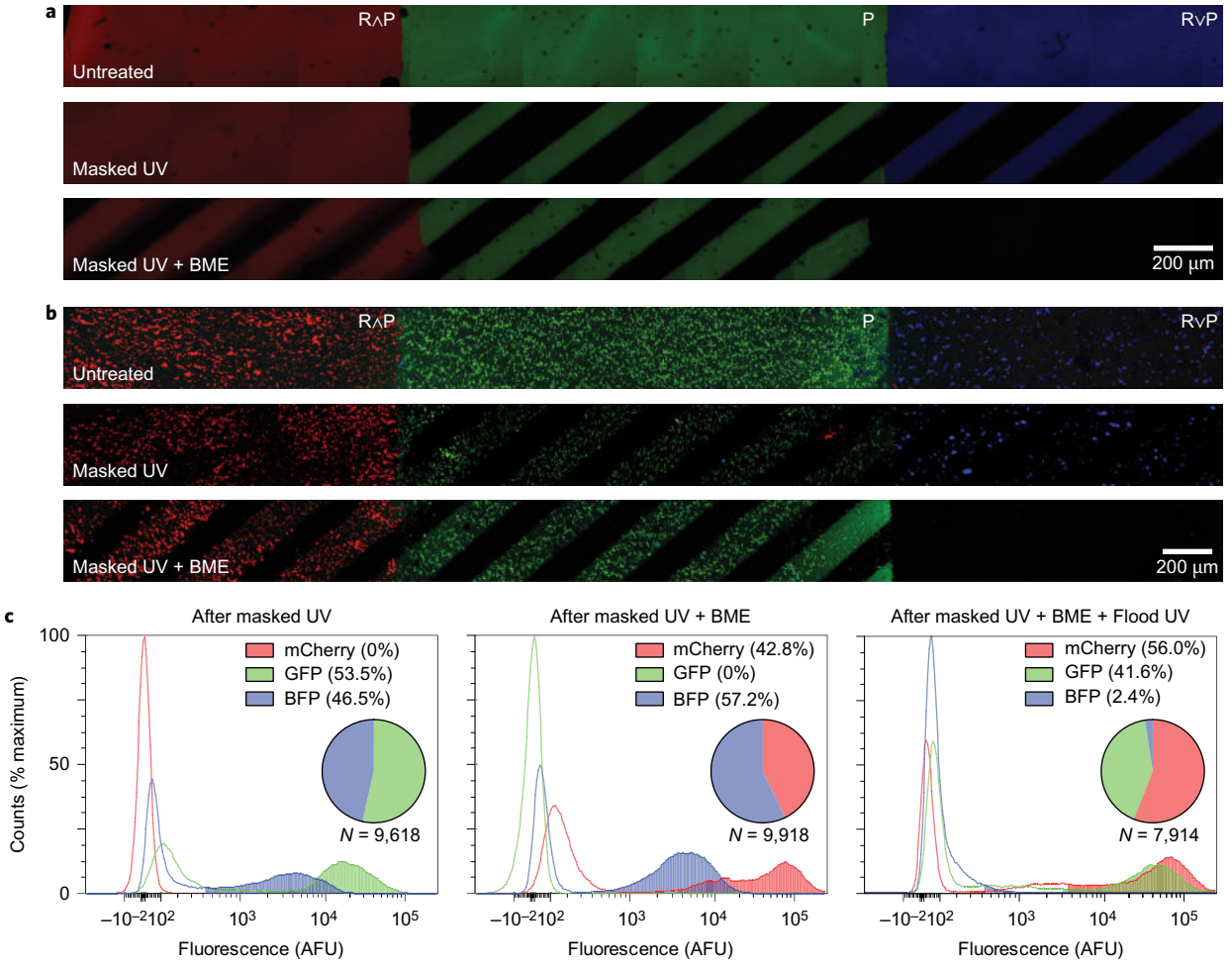

Figure 5 | Sequential and spatiotemporally varied delivery of small molecules and cells from gels following logic-based response to environmental cues. **a**, Spatially segregated regions of fluorescently labelled RΛP (red), P (green) and RVP (blue) were formulated and imaged by confocal microscopy following sequential treatments of photomasked light and reducing conditions (β-mercaptoethanol, BME). Each region responded to the cues as engineered, degrading only in the presence of the proper set of input conditions. Scale bar, 200 μm. **b**, The experiment in **a** was repeated with encapsulated fluorescent cells (hS5 stably transfected to produce mCherry, green fluorescent protein (GFP) and blue fluorescent protein (BFP), respectively, replacing the small molecule fluorophores). Scale bars, 200 μm. **c**, Cells released from gels in **b** following sequential exposure to photomasked UV light, reducing conditions and UV light flood exposure were quantified using flow cytometry. Histograms present fluorescence intensity for channels corresponding to each cell line, with shaded regions indicating positively gated cells. AFU, arbitrary fluorescent units.

logic-based gel degradation, enabling precise regulation of cell fate in response to disease-defined combinations of external cues.

Logic-based delivery of live cells from stimuli-responsive hydrogels. To illustrate the biocomputational response of these engineered materials to a combination of spatially defined as well as environmental cues, we formulated a multifunctional hydrogel composed of three distinct logic regions (RΛP, P, RVP), each labelled with a different fluorophore (Fig. 5). These hydrogels were sequentially exposed to masked UV light and reducing conditions, and imaged using fluorescent confocal microscopy (Supplementary Methods 30). Each region responded to external cues as engineered, degrading only when the proper set of input conditions was presented. To demonstrate cytocompatible gelation and multi-stimuli-responsive degradation, an analogous experiment was performed with each region containing encapsulated hS5 bone marrow-derived stromal cells that constitutively express a different fluorescent protein. Cells were released from gels following sequential masked light exposure, reducing conditions and flood illumination, harvested after each treatment, and analysed by flow cytometry. Each treatment yielded a distinct cell collection matching the expected colour composition (Supplementary Methods 31). Encapsulated cells were also shown to be viable when released through each stimulus, demonstrating whole process cytocompatibility (Supplementary Fig. 12). This material system, which yields the sequential and environmentally triggered release of multiple cell lines in well-defined combinations, is the most advanced live-cell delivery platform realized so far.

Discussion

Although we have first implemented our logic-gated approach to control biomaterial degradation using SPAAC-based PEG hydrogels that respond to reductant, enzyme and light inputs, these general methodologies should be readily extendable to different stimuli-labile moieties, polymer compositions and gelation chemistries. We hypothesize that these logic-based strategies can be extended to covalently tether other small molecules, peptides, proteins, polysaccharides and nucleic acids to a non-degradable hydrogel via a stimuli-responsive linker, affording precise biochemical presentation through environmentally triggered controlled release of bioactive species.

Another potential benefit of our approach stems from the ability to tailor the 'propagation delay' (the time required to transduce

input signals into the appropriate functional output) of the Boolean operator for different therapeutic applications. For these logic-based materials, gate delay is governed by the susceptibility of each labile region to its relevant input, overall construct size/geometry, and the concentrations of the environmental cues triggering degradation. The degradation rate of a linkage to a given input may be tuned over several orders of magnitude, for example by modifying substituents on photodegradable groups or substituting single amino acids within enzyme-labile peptide sequences[24,35–37]. The propagation delay can be further decreased by formulating materials into geometries where response is reaction-limited rather than diffusion-limited. Careful choice of construct geometry and stimuli-labile group identity enables user-specified control over material response rates.

Capitalizing on this platform's unique capacity to govern material properties in response to combinations of both exogenous user-specified spatiotemporal cues (such as light) and endogenous cell-produced signals (such as enzymes and reductants) may enable new advances in three-dimensional (3D) cell culture and tissue engineering. In one envisioned application, user-specified material photodegradation can be performed within E∨P gels to generate customizable vasculature[38] within a synthetic environment that supports enzyme-mediated matrix remodelling and long-term cell survival. In another, cells encapsulated within a photopatterned E∧P material will only undergo cell-mediated spreading within user-defined gel regions. We anticipate that such combined user and cellular control over the culture microenvironment will provide unique opportunities towards directing 4D stem cell differentiation[29,39,40].

Here we have introduced the first modular approach to engineer materials with tailored, user-specified, logic-based responsiveness to environmental cues. By controlling the molecular architecture and connectivity of multiple stimuli-labile moieties within discrete peptide-based cross-linkers, we have endowed biomaterials with unprecedented computational capacity through hierarchical combinations of Boolean YES/OR/AND gates. Having exhaustively synthesized cross-linkers that are each uniquely sensitive to combinations of three orthogonal inputs (enzyme, reductant and light), we have shown that constructs exhibit expected behaviour spanning molecular and macroscopic scales. We have utilized these platforms to demonstrate the first sequential and spatiotemporally varied delivery of multiple cell lines from a single gel, as well as the controlled release of a functional chemotherapeutic in response to disease-associated cues. We expect that these platforms will find great utility in targeted drug delivery, where release of therapeutics, proteins and cells can be confined to sites of disease with high selectivity, as well as in applications for diagnostics, tissue engineering and regenerative medicine.

Methods

Synthesis and characterization of logic cross-linkers. For complete details of all logic cross-linker syntheses and characterization, see Supplementary Methods 1–21. Briefly, peptides were generated by standard microwave-assisted Fmoc solid-phase peptide synthesis (CEM Liberty 1) and purified using reversed-phase high-pressure liquid chromatography (RP-HPLC, Dionex Ultimate 3000, C18 column). Peptide-based cross-linkers were characterized by MALDI–TOF mass spectrometry (Bruker AutoFlex II).

Assessing solution-based cross-linker degradation in response to external stimuli. Each cross-linker species (40 nmol) was dissolved in MMP buffer (110 µl, 200 mM sodium chloride, 50 mM tris, 5 mM calcium chloride, 1 µM zinc chloride, pH adjusted to 7.5 with hydrochloric acid) and exposed to each unique combination of enzyme, reductant and light.

Samples receiving the reductive input ($_R$) were treated with tris(2-carboxyethyl) phosphine hydrochloride (TCEP·HCl, 200 nmol) and all samples were incubated overnight (37 °C). To quench any unreached TCEP, these samples were further treated with hydroxyethyl disulfide (HEDS, 500 nmol) and incubated (4 h, 37 °C). Samples receiving the enzyme input ($_E$) were then treated with MMP-8 (5 µl, 0.2 mg ml^{-1} in MMP buffer) and all samples were incubated overnight (37 °C). Samples receiving the light input ($_P$) were subsequently exposed to UV light (λ = 365 nm, 10 mW cm^{-2} incident light, 60 min). All samples were diluted with acetonitrile/water (20:80, 100 µl) containing trifluoroacetic acid (0.1%) and characterized by MALDI–TOF. Mass-to-charge ratios (m/z) of treated species were compared to expected products (Supplementary Figs 1–9). Complete experimental details are provided in Supplementary Methods 24.

***In situ* rheology of hydrogel formation.** Oscillatory rheological analysis (Anton Paar MCR301) was performed with a cone and plate geometry (25 mm diameter, 1° cone) at 25 °C and 25 Hz with 1% strain (conditions identified to be in the viscoelastic region). The E∧P cross-linker was pre-treated with each combination of MMP ($_E$) and/or light ($_P$), as described above. A hydrogel precursor solution of PEG-tetraBCN (2 mM) and pre-treated E∧P cross-linker (4 mM) in MMP buffer was reacted *in situ*, and G' and G'' were monitored for 120 min. Complete experimental details are provided in Supplementary Methods 25.

Logic-based hydrogel degradation in response to sequential stimuli. Fluorescent hydrogels (10 µl) were formulated in microcentrifuge tubes from a precursor solution of PEG-tetraBCN-AF568 (2 mM) and a logic peptide cross-linker (4 mM) in MMP buffer (reacted for 60 min, 25 °C). Hydrogels were washed in MMP buffer. Every logic material was treated with each unique input combination in experimental triplicate, as described above. The extent of gel degradation was assessed by supernatant fluorescence quantification (SpectraMax M5: excitation, 570 nm; emission, 610 nm; emission cutoff filter, 590 nm). Complete experimental details are provided in Supplementary Methods 27.

***In vitro* cellular response to environmentally triggered degradation of a doxorubicin hydrogel.** Hydrogels (15 µl) were formulated with DOX (1 mM) from a precursor solution of PEG-tetraBCN (2 mM) and the R∧E-DOX linker (4 mM, Supplementary Methods 29) in HEPES buffer (5 mM HEPES, 3 mM $CaCl_2$, 5 µM $ZnCl_2$). Gels were washed with HEPES buffer and treated with each set of relevant inputs in experimental triplicate. Hydrogel supernatant was collected and diluted (1:1) with 2× Dulbecco's modified Eagle's medium. HeLa cells were cultured in this mixture (170 µl) in a 96-well plate for 48 h (beginning 24 h after HeLa seeding at 2×10^3 cells per well), after which cellular dsDNA content was quantified with a PicoGreen Assay (ThermoFisher). Complete experimental details are provided in Supplementary Methods 29.

Multi-logic hydrogel treatment and visualization. Hydrogels (130 µm thickness) were formulated with three distinct logically degradable regions, each labelled with a unique fluorophore: (1) R∧P cross-linker with AF568; (2) P cross-linker with 5-carboxyfluorescein (FAM); and (3) R∨P cross-linker with Cyanine5.

Hydrogels were imaged by fluorescent confocal microscopy. Preformed tri-colour gels were exposed to UV light (λ = 365 nm, 10 mW cm^{-2} incident light, 10 min) through a slitted photomask (alternating 200 µm wide lines and spaces) and imaged. Gels were subsequently treated with 2-mercaptoethanol (BME, 0.25 mM in 50 ml phosphate-buffered saline (PBS), 45 min, 25 °C) and imaged. Complete experimental details are provided in Supplementary Methods 30.

Hydrogel-encapsulated cell release studies. Hydrogels (130 µm thickness) were formulated with three distinct logically degradable regions, each encapsulating an hS5 cell line (40×10^6 cells ml^{-1}) that stably expresses a unique fluorescent protein: (1) R∧P cross-linker with hS5-mCherry$^+$; (2) P cross-linker with hS5-GFP$^+$; and (3) R∨P cross-linker with hS5-BFP$^+$. Cell-laden hydrogels were incubated overnight in medium (RPMI-1640, 10% fetal bovine serum, 1% penicillin–streptomycin). Hydrogels were treated sequentially with light and reducing conditions, and imaged as described above.

Following each degradative step, released cells were collected and fixed (4% formaldehyde). Flow cytometry was performed on released cell populations (BD Biosciences LSR II Flow Cytometer). Forward scattering, side scattering and fluorescence corresponding to each protein were recorded for each event. Complete experimental and analytical details are provided in Supplementary Methods 31.

Cell viability following hydrogel encapsulation and triggered release. hS5 cells (40×10^6 cells ml^{-1}) were encapsulated within each single-input responsive hydrogel (130 µm thick, either R, E or P) in experimental triplicate, and stored in medium for 1 h. To induce gel degradation, R gels were treated with BME (0.25 mM in PBS, 37 °C, 45 min), P gels were exposed to UV light (λ = 365 nm, 10 mW cm^{-2}, 10 min), and E gels were treated with MMP-8 (0.20 nM in RPMI, 37 °C, 60 min). Cells were collected, stained with a Live/Dead assay (Invitrogen) and imaged (Nikon Eclipse TE2000-U). Cell viability was determined by standard image analysis. Complete experimental details are provided in Supplementary Fig. 12.

Life Sciences Reporting Summary. Further information on experimental design and reagents is available in the Life Sciences Reporting Summary.

Data availability. The characterization data and experimental protocols for this work are available within this manuscript and its associated Supplementary Information, or from the corresponding author upon request.

Received 19 December 2016; accepted 17 November 2017; published online 15 January 2018

References

1. Burdick, J. A. & Murphy, W. L. Moving from static to dynamic complexity in hydrogel design. *Nat. Commun.* **3,** 1269 (2012).
2. Hoffman, A. S. Stimuli-responsive polymers: biomedical applications and challenges for clinical translation. *Adv. Drug Deliv. Rev.* **65,** 10–16 (2013).
3. Knipe, J. M. & Peppas, N. A. Multi-responsive hydrogels for drug delivery and tissue engineering applications. *Regen. Biomater.* **1,** 57–65 (2014).
4. Mura, S., Nicolas, J. & Couvreur, P. Stimuli-responsive nanocarriers for drug delivery. *Nat. Mater.* **12,** 991–1003 (2013).
5. O'Neill, H. S. *et al.* Biomaterial-enhanced cell and drug delivery: lessons learned in the cardiac field and future perspectives. *Adv. Mater.* **28,** 5648–5661 (2016).
6. Tibbitt, M. W., Rodell, C. B., Burdick, J. A. & Anseth, K. S. Progress in material design for biomedical applications. *Proc. Natl Acad. Sci. USA* **112,** 14444–14451 (2015).
7. Evans, A. C., Thadani, N. N. & Suh, J. Biocomputing nanoplatforms as therapeutics and diagnostics. *J. Control. Rel.* **240,** 387–393 (2016).
8. Lu, Y., Aimetti, A. A., Langer, R. & Gu, Z. Bioresponsive materials. *Nat. Rev. Mater.* **2,** 16075 (2016).
9. DeForest, C. A. & Anseth, K. S. Advances in bioactive hydrogels to probe and direct cell fate. *Annu. Rev. Chem. Biomol. Eng.* **3,** 421–444 (2012).
10. Li, J. & Mooney, D. J. Designing hydrogels for controlled drug delivery. *Nat. Rev. Mater.* **1,** 16071 (2016).
11. McCawley, L. J. & Matrisian, L. M. Matrix metalloproteinases: multifunctional contributors to tumor progression. *Mol. Med. Today* **6,** 149–156 (2000).
12. Chen, X. *et al.* Dual bioresponsive mesoporous silica nanocarrier as an 'AND' logic gate for targeted drug delivery cancer cells. *Adv. Funct. Mater.* **24,** 6999–7006 (2014).
13. Choh, S., Cross, D. & Wang, C. Facile synthesis and characterization of disulfide-cross-linked hyaluronic acid hydrogels for protein delivery and cell encapsulation. *Biomacromolecules* **12,** 1126–1136 (2011).
14. Douglas, S. M., Bachelet, I. & Church, G. M. A logic-gated nanorobot for targeted transport of molecular payloads. *Science* **335,** 831–834 (2012).
15. Ikeda, M. *et al.* Installing logic-gate responses to a variety of biological substances in supramolecular hydrogel-enzyme hybrids. *Nat. Chem.* **6,** 511–518 (2014).
16. Komatsu, H. *et al.* Supramolecular hydrogel exhibiting four basic logic gate functions to fine-tune substance release. *J. Am. Chem. Soc.* **131,** 5580–5585 (2009).
17. Liu, G., Ji, W. & Feng, C. Installing logic gates to multiresponsive supramolecular hydrogel co-assembled from phenylalanine amphiphile and bis(pyridinyl) derivative. *Langmuir* **31,** 7122–7128 (2015).
18. Motornov, M. *et al.* 'Chemical transformers' from nanoparticle ensembles operated with logic. *Nano Lett.* **8,** 2993–2997 (2008).
19. Kharkar, P. M., Kiick, K. L. & Kloxin, A. M. Design of thiol- and light-sensitive degradable hydrogels using Michael-type additon reactions. *Polym. Chem.* **6,** 5565–5574 (2015).
20. de Garcia Lux, C. *et al.* Short soluble coumarin crosslinkers for light-controlled release of cells and proteins from hydrogels. *Biomacromolecules* **16,** 3286–3296 (2015).
21. Roche, E. T. *et al.* Comparison of biomaterial delivery vehicles for improving acute retention of stem cells in the infarcted heart. *Biomaterials* **35,** 6850–6858 (2014).
22. Steinhilber, D. *et al.* A microgel construction kit for bioorthogonal encapsulation and pH-controlled release of living cells. *Angew. Chem. Int. Ed.* **52,** 13538–13543 (2013).
23. Griffin, D. R. & Kasko, A. M. Photodegradable macromers and hydrogels for live cell encapsulation and release. *J. Am. Chem. Soc.* **134,** 13103–13107 (2012).
24. Nagase, H. & Fields, G. B. Human matrix metalloproteinase specificity studies using collagen sequence-based synthetic peptides. *Pept. Sci.* **40,** 399–416 (1996).
25. Kloxin, A. M., Tibbitt, M. W. & Anseth, K. S. Synthesis of photodegradable hydrogels as dynamically tunable cell culture platforms. *Nat. Protoc.* **5,** 1867–1887 (2010).
26. Agard, N. J., Prescher, J. A. & Bertozzi, C. R. A strain-promoted [3+2] azide–alkyne cycloaddition for covalent modification of biomolecules in living systems. *J. Am. Chem. Soc.* **126,** 15046–15047 (2004).
27. DeForest, C. A. & Anseth, K. S. Cytocompatible click-based hydrogels with dynamically tunable properties through orthogonal photoconjugation and photocleavage reactions. *Nat. Chem.* **3,** 925–931 (2011).
28. DeForest, C. A., Polizzotti, B. D. & Anseth, K. S. Sequential click reactions for synthesizing and patterning three-dimensional cell microenvironments. *Nat. Mater.* **8,** 659–664 (2009).
29. DeForest, C. A. & Tirrell, D. A. A photoreversible protein-patterning approach for guiding stem cell fate in three-dimensional gels. *Nat. Mater.* **14,** 523–531 (2015).
30. Madl, C. M., Katz, L. M. & Heilshorn, S. C. Bio-orthogonally crosslinked, engineered protein hydrogels with tunable mechanics and biochemistry for cell encapsulation. *Adv. Funct. Mater.* **26,** 3612–3620 (2016).
31. Jiang, Y., Chen, J., Deng, C., Suuronen, E. J. & Zhong, Z. Click hydrogels, microgels and nanogels: emerging platforms for drug delivery and tissue engineering. *Biomaterials* **35,** 4969–4985 (2014).
32. Das, R. K., Gocheva, V., Hammink, R., Zouani, O. F. & Rowan, A. E. Stress-stiffening-mediated stem-cell commitment switch in soft responsive hydrogels. *Nat. Mater.* **15,** 318–325 (2016).
33. Hiemenz, P. C. & Lodge, T. P. *Polymer Chemistry* (CRC Press, 2007).
34. Flynn, B. P. *et al.* Mechanical strain stabilizes reconstituted collagen fibrils against enzymatic degradation by mammalian collagenase matrix metalloproteinase 8 (MMP-8). *PLoS ONE* **5,** e12337 (2010).
35. Huo, M., Yuan, J. & Wei, Y. Redox-responsive polymers for drug delivery: from molecular design to applications. *Polym. Chem.* **5,** 1519–1528 (2014).
36. Zhu, C., Ninh, C. & Bettinger, C. J. Photoreconfigurable polymers for biomedical applications: chemistry and macromolecular engineering. *Biomacromolecules* **15,** 3474–3494 (2014).
37. Uhrich, K. E., Cannizzaro, S. M., Langer, R. S. & Shakesheff, K. M. Polymeric systems for controlled drug release. *Chem. Rev.* **99,** 3181–3198 (1999).
38. Arakawa, C. K., Badeau, B. A., Zheng, Y. & DeForest, C. A. Multicellular vascularized engineered tissues through user-programmable biomaterial photodegradation. *Adv. Mater.* **29,** 1703156 (2017).
39. Khetan, S. & Burdick, J. A. Patterning network structure to spatially control cellular remodeling and stem cell fate within 3-dimensional hydrogels. *Biomaterials* **31,** 8228–8234 (2010).
40. Khetan, S. *et al.* Degradation-mediated cellular traction directs stem cell fate in covalently crosslinked three-dimensional hydrogels. *Nat. Mater.* **12,** 458–465 (2013).

Acknowledgements

The authors thank B. Hayes and B. Torok-Storb for gifting the hS5 cells, S. Adelmund for synthesizing and supplying BCN-OSu, E. Ruskowitz for useful discussion involving the DOX studies, as well as K. Anseth, D. Tirrell, S. Pun and B. Ratner for constructive comments during the preparation of this manuscript. The authors acknowledge support from S. Edgar at the University of Washington (UW) Mass Spectrometry Center, D. Prunkard at the UW Pathology Flow Cytometry Core Facility, and N. Peters and support from the NIH to the UW W. M. Keck Microscopy Center (S10 OD016240). This work was supported by a University of Washington Faculty Startup Grant (to C.A.D.) and a National Science Foundation CAREER Award (DMR 1652141, to C.A.D.).

Author contributions

B.A.B. and C.A.D. conceived and designed the experiments. B.A.B., M.P.C., C.K.A. and J.A.S. performed the experiments. B.A.B. and C.A.D. analysed the data and prepared the figures. B.A.B. and C.A.D. wrote the paper.

Additional information

Supplementary information is available in the online version of the paper. Reprints and permissions information is available online at www.nature.com/reprints. Publisher's note: Springer Nature remains neutral with regard to jurisdictional claims in published maps and institutional affiliations. Correspondence and requests for materials should be addressed to C.A.D.

Competing financial interests

The authors declare no competing financial interests.